

Vitamin B12 and folic acid alleviate symptoms of nutritional deficiency by antagonizing aryl hydrocarbon receptor

Daniel J. Kim^a, Arvind Venkataraman^a, Priyanka Caroline Jain^a, Eleanor P. Wiesler^a, Melody DeBlasio^a, Jonathan Klein^a, Stephanie S. Tu^a, Seohyuk Lee^a, Ruslan Medzhitov^{a,b}, and Akiko Iwasaki^{a,b,1}

^aDepartment of Immunobiology, Yale University School of Medicine, New Haven, CT 06520; and ^bHoward Hughes Medical Institute, Yale University School of Medicine, New Haven, CT 06520

Contributed by Akiko Iwasaki, May 16, 2020 (sent for review April 13, 2020; reviewed by Daniel Mucida and Francisco J. Quintana)

Despite broad appreciation of their clinical utility, it has been unclear how vitamin B12 and folic acid (FA) function at the molecular level to directly prevent their hallmark symptoms of deficiency like anemia or birth defects. To this point, B12 and FA have largely been studied as cofactors for enzymes in the one-carbon (1C) cycle in facilitating the de novo generation of nucleotides and methylation of DNA and protein. Here, we report that B12 and FA function as natural antagonists of aryl hydrocarbon receptor (AhR). Our studies indicate that B12 and FA bind AhR directly as competitive antagonists, blocking AhR nuclear localization, XRE binding, and target gene induction mediated by AhR agonists like 2,3,7,8-tetrachlorodibenzodioxin (TCDD) and 6-formylindolo[3,2-b]carbazole (FICZ). In mice, TCDD treatment replicated many of the hallmark symptoms of B12/FA deficiency and cotreatment with aryl hydrocarbon portions of B12/FA rescued mice from these toxic effects. Moreover, we found that B12/FA deficiency in mice induces AhR transcriptional activity and accumulation of erythroid progenitors and that it may do so in an AhR-dependent fashion. Consistent with these results, we observed that human cancer samples with deficient B12/FA uptake demonstrated higher transcription of AhR target genes and lower transcription of pathways implicated in birth defects. In contrast, there was no significant difference observed between samples with mutated and intact 1C cycle proteins. Thus, we propose a model in which B12 and FA blunt the effect of natural AhR agonists at baseline to prevent the symptoms that arise with AhR overactivation.

vitamin | folic acid | AhR | birth defect | nutrition

Deficiencies in vitamin B12 and folate (folic acid [FA]) are some of the most prevalent nutritional deficiencies in the world, affecting more than 30% and 20% of the population, respectively, in some developing countries (1, 2). Particularly common among elderly, pregnant, and vegan populations (2, 3), these deficiencies present with megaloblastic anemia (4), birth defects (including neural tube defects and cleft palates) (5, 6), and chronic liver disease (7), among other comorbidities. Fortunately, these consequences of vitamin deficiency can be easily prevented by dietary supplementation. In fact, over 80 countries worldwide have mandatory folate fortification laws in place, and it is estimated that, in the United States alone, these laws save the US health care system up to \$600 million every year through the prevention of birth defects like spina bifida (8).

Despite such successful policy interventions, however, the molecular mechanism underlying the pathophysiology of B12/FA deficiency still remains unclear. On one hand, B12 and FA are already known to act as cofactors for methionine synthase (MS) and methylenetetrahydrofolate reductase (MTHFR), respectively, in the 1-carbon (1C) cycle, supplying methyl groups for de novo nucleotide synthesis and DNA/protein methylation (9). From here, it has been largely assumed that the symptoms arising with B12/FA deficiency, especially birth defects, arise directly from faulty DNA synthesis (10). This explanation, however, does not

sufficiently account for why birth defects tend to be so focal in their presentation—narrowly affecting one organ system while preserving others—despite the fact that all cell types would require new DNA for division at such an early embryonic age. Furthermore, mice deficient in MTHFR and MS do not phenocopy classic symptoms of B12/FA deficiency: MTHFR^{-/-} and MS^{+/-} mice do not show anemia or birth defects, and MS^{-/-} embryos were all found to die shortly after implantation (11–13), a far more deleterious phenotype than seen with B12/FA deficiency. These shortcomings raise the possibility that B12/FA may be engaging another pathway to directly control physiological processes like hematopoiesis or embryonic development.

Given that B12 and FA both contain aryl hydrocarbon rings that have not yet been functionally elucidated (Fig. 1A), we hypothesized that these vitamins, formed exclusively by bacteria, might act as ligands for the aryl hydrocarbon receptor (AhR), a xenobiotic receptor that activates a pleiotropic transcriptional response after binding ligands containing aryl hydrocarbon rings. In addition to up-regulating genes like *CYP1A1* that encode detoxifying P450 enzymes, AhR is known to drive many developmental and homeostatic processes at baseline by responding to natural agonists (14). By selectively activating AhR, prototypical agonists like 2,3,7,8-tetrachlorodibenzodioxin

Significance

Vitamin B12 and folic acid (FA) deficiencies present with symptoms like anemia and birth defects, but the underlying mechanism remains unclear. Here, we show that B12 and FA antagonize aryl hydrocarbon receptor (AhR), which has been implicated in anemia and birth defects. We found that treatments with B12/FA rescued mice from AhR agonist-mediated anemia, fatty livers, and cleft palates. B12/FA-deficient mice exhibited higher AhR transcriptional activity and faulty erythropoiesis that were abrogated with AhR deficiency. Last, we verified that human samples lacking functional B12/FA uptake exhibit higher expression of AhR target genes and lower transcription of pathways implicated in birth defects. Our study provides a parsimonious explanation for how deficiency symptoms arise and informs other comorbidities driven by AhR hyperstimulation.

Author contributions: D.J.K., A.V., R.M., and A.I. designed research; D.J.K., A.V., P.C.J., E.P.W., M.D., J.K., S.S.T., and S.L. performed research; D.J.K. and A.V. contributed new reagents/analytic tools; D.J.K., A.V., P.C.J., E.P.W., M.D., J.K., S.S.T., R.M., and A.I. analyzed data; and D.J.K. and A.I. wrote the paper.

Reviewers: D.M., Rockefeller University; and F.J.Q., Brigham and Women's Hospital, Harvard Medical School.

The authors declare no competing interest.

Published under the PNAS license.

¹To whom correspondence may be addressed. Email: akiko.iwasaki@yale.edu.

This article contains supporting information online at <https://www.pnas.org/lookup/suppl/doi:10.1073/pnas.2006949117/-DCSupplemental>.

First published June 22, 2020.

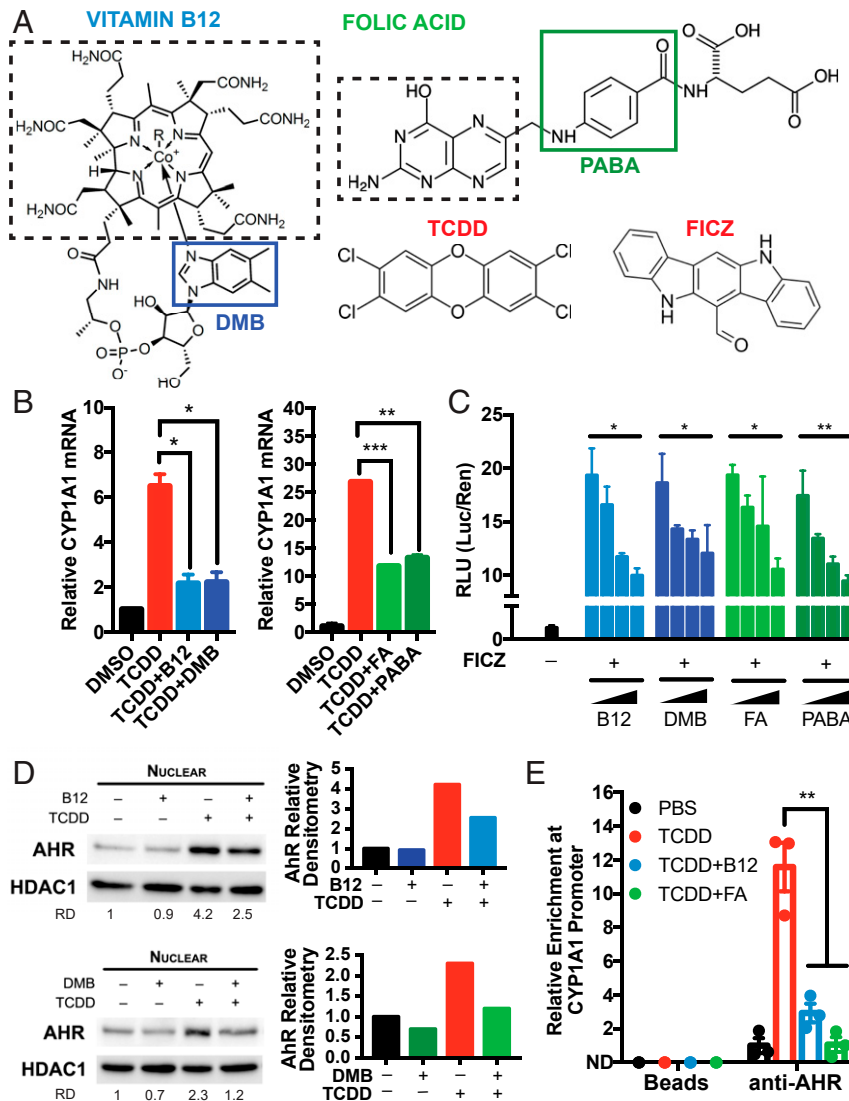


Fig. 1. B12 and FA suppress AhR transcriptional activity induced by AhR agonists. (A) Chemical structures of vitamin B12 and folic acid (FA) alongside prototypical AhR agonists TCDD and FICZ. The solid boxes indicate the moieties of B12 and FA that contain aryl hydrocarbon rings: DMB and PABA, respectively. The dashed boxes indicate portions of B12 and FA that are involved in methyl donation in the 1C cycle. (B) HepG2 human hepatoma cells were pretreated with 5,000 pg/mL B12 (with recombinant B12 carrier protein 5 pM TCN2), 3.4 nM DMB, 50 ng/mL FA, or 113 nM PABA for 8 h and treated with 0.5 nM TCDD for 5 h. Relative *CYP1A1* mRNA was measured by RT-qPCR and normalized to *HPRT1* and DMSO-treated samples. Data are means \pm SE ($n = 2$). * $P < 0.05$, ** $P < 0.01$, and *** $P < 0.001$ vs. TCDD-treated samples assessed by Student's t test. (C) HepG2 cells were transfected with pGL4.43 XRE-luc2P and pGL4.75 CMV-Ren plasmids for 24 h, pretreated with serial 100-fold dilutions of B12/TCN2 (maximum [max] concentration: 5,000 pg/mL B12 with 5 pM TCN2), DMB (max, 3.4 nM DMB), FA (max, 50 ng/mL), or PABA (max, 113 nM) for 8 h, and treated with 1 nM FICZ for 12 h. Luminescence from cell lysates were measured by commercial kit and analyzed by microplate reader. Relative luciferase units (RLUs) were calculated by normalizing firefly luciferase signal with *Renilla* luciferase signal within each sample and further normalizing with DMSO-treated samples. * $P < 0.05$, ** $P < 0.01$ assessed by linear regression of RLU vs. log(concentration). (D) HepG2 cells were treated with 0.5 nM TCDD in the presence of 5,000 pg/mL B12 (with 5 pM TCN2) or 3.4 nM DMB for 24 h. Nuclear expressions of AhR and HDAC1 were measured by Western blotting. Relative densitometry (RD) of AhR blots were quantified by ImageJ. (E) HepG2 cells were treated with 0.5 nM TCDD in the presence of 5,000 pg/mL B12 (with 5 pM TCN2) and 50 ng/mL FA for 2 h. Chromatin immunoprecipitation (ChIP) was performed with anti-AhR antibodies and protein G magnetic beads. Binding at the putative AhR binding site *CYP1A1* promoter was measured by RT-qPCR and normalized to 5% input. Data are means \pm SE ($n = 3$). ** $P < 0.01$ vs. TCDD-treated samples assessed by Student's t test.

(TCDD) (also commonly known as dioxin) have proven to be a valuable molecular tool in identifying some of these biological functions. For instance, longitudinal clinical studies following patients exposed to dioxin and related animal studies have demonstrated that AhR overactivation can cause macrocytic anemia (15, 16), neural tube defects (17, 18), cleft palate (19), and fatty liver disease (20, 21).

Given the clinical similarities between AhR hyperstimulation and B12/FA deficiency, we examined whether B12 and FA might function as AhR antagonists to counteract natural AhR agonists

present at baseline (e.g., 6-formylindolo[3,2-b]carbazole [FICZ], ITE, or kynurenic acid). Here, we show that B12 and FA bind directly to AhR and suppress transcriptional activation by prototypical agonists. We demonstrate that treatment with the aryl hydrocarbon moieties of B12/FA is sufficient in rescuing mice from classic symptoms of vitamin deficiency and those induced by TCDD and further show that B12- and FA-deficient diets induce AhR transcriptional activity, in an AhR-dependent fashion. Last, we report here that human deficiency in B12/FA uptake, but not in 1C metabolism, is associated with a relative induction in

AhR activity and repression in pathways associated with birth defect. Together, these results offer a model of vitamin B12 and FA deficiency, centered around AhR, that explains the classic symptoms and comorbidities of deficiency in a parsimonious way.

Results

B12 and FA Inhibit AhR Transcriptional Activity Induced by Known Agonists. To begin assessing the putative impact of B12 and FA on AhR signaling, we utilized HepG2 human hepatoma cells, which express high AhR at baseline and are commonly used to characterize novel AhR ligands. After culturing cells in serum-starved media to minimize background B12 and FA, we pretreated HepG2 cells with vitamin B12 (with required B12 carrier TCN2) and FA for 8 h, treated with TCDD for 5 h, and measured *CYP1A1* mRNA with RT-qPCR as a readout of AhR transcriptional activity. While TCDD alone significantly induced *CYP1A1* mRNA as expected, pretreatment with physiologically relevant concentrations of B12 and FA (at nanomolar quantities) significantly reduced *CYP1A1* mRNA (Fig. 1B). Furthermore, we found that treatments with equimolar amounts of 5,6-dimethylbenzimidazole (DMB) and *para*-aminobenzoic acid (PABA)—the aryl hydrocarbon portions of B12 and FA, respectively (Fig. 1A)—were sufficient in replicating this effect (Fig. 1B).

To assess whether this suppression is being mediated through AhR, we cotransfected HepG2 cells with a plasmid expressing firefly luciferase under the control of a minimal promoter containing three copies of putative AhR binding sites, xenobiotic response elements (XREs), and another plasmid constitutively expressing *Renilla* luciferase. Dual luciferase assays revealed that B12, DMB, FA, and PABA were all able to suppress AhR signaling induced by FICZ, another AhR agonist, in a dose-dependent fashion (Fig. 1C). Interestingly, with supraphysiologic concentrations in the same experiment (i.e., 50 times greater than the upper range of physiologic B12/FA serum concentrations), the antagonistic effects of compounds appeared to diminish, suggesting the possibility of a U-shaped relationship at extremely high doses (*SI Appendix*, Fig. S1A).

Because the ligand binding domain (LBD) of AhR is relatively wide and open, synthetic antagonists like CH-223191 are able to block the activation of certain classes of AhR ligands that include TCDD, but not others like polycyclic aromatic hydrocarbons (PAHs), which include the agonist benzopyrene (BaP) (22). To test whether B12/FA behaves similarly to synthetic antagonists, we performed dual luciferase assays with BaP and found that B12, DMB, FA, and PABA were unable to suppress BaP-induced transcriptional activity (*SI Appendix*, Fig. S2). These results suggest that the antagonism is being mediated through specific residues in the LBD and not by any extrinsic mechanism, such as altered interactions with chaperone proteins or global hypermethylation.

Next, we measured AhR localization in nuclear lysate by Western blotting and found that treatments with B12 or DMB suppressed nuclear localization of AhR (Fig. 1D). We observed similar results with FA and PABA, although this conclusion is somewhat limited by variations in loading control (*SI Appendix*, Fig. S3). In line with this inhibition of nuclear localization, chromatin immunoprecipitation (ChIP) revealed that B12/FA abrogated AhR enrichment at an XRE within the *CYP1A1* promoter (Fig. 1E). In sum, these results indicate that B12 and FA selectively block the activation of AhR by TCDD and FICZ and that their respective aryl hydrocarbon ring moieties are sufficient to mediate this block.

B12 and FA Bind AhR Directly to Compete with TCDD. To examine whether vitamin B12 and FA engage AhR directly, we first performed a dual luciferase assay to generate dose-response curves for TCDD in the presence of vitamins and their aryl hydrocarbon ring moieties. We observed that physiologically relevant concentrations of the compounds were sufficient in producing a right shift in the EC₅₀ of TCDD (Fig. 2A). The fact

that their antagonism could be abrogated with sufficiently saturating concentrations of agonist suggests that these compounds are indeed acting competitively at the LBD of AhR.

Next, to measure direct binding to AhR, we transitioned to a cell-free system by collecting lysate from HEK293T cells over-expressing human AhR and probing with streptavidin beads conjugated to biotinylated-B12 or biotinylated-FA (*SI Appendix*, Fig. S4). Western blot of the eluted protein revealed significant binding of AhR to B12 was subsequently quenched with increasing concentrations of TCDD (Fig. 2B). Particularly by comparing lanes 10 and 12, FA also appears to show a similar effect, although this conclusion is limited by the quality of the blots (Fig. 2B).

We confirmed this binding interaction through a complementary enzyme-linked immunosorbent assay (ELISA) approach that immobilizes AhR with antibody and measures binding of biotinylated-B12 and biotinylated-FA with streptavidin-HRP (Fig. 2C). In this ELISA-based system, we also found that the binding between AhR and the vitamins could be outcompeted with high concentrations of TCDD (Fig. 2D) and DMB or PABA (Fig. 2E). While a nonaromatic biotinylated small molecule would provide better control for specificity than free biotin, our competition studies with TCDD—given the wide use of similar experiments in the AhR field (23)—still provide strong support for specific binding of vitamins at the LBD of AhR. Indeed, our data further suggest that this binding may occur through their aryl hydrocarbon ring moieties.

DMB and PABA Rescue Symptoms of Vitamin Deficiency Induced by TCDD. We were next interested in testing whether B12 and FA could antagonize AhR activity *in vivo* and rescue mice from symptoms of B12/FA deficiency induced by TCDD.

TCDD has already been described to induce various hematologic abnormalities in mice, including macrocytic anemia and thrombocytopenia (16). In our studies, treatment with B12, FA, or their aryl hydrocarbon ring moieties not only suppressed *Cyp1a1* mRNA induction (Fig. 3A and *SI Appendix*, Fig. S5A), but also rescued mice from anemia and thrombocytopenia induced by TCDD and FICZ (Fig. 3B and *SI Appendix*, Fig. S5B). To verify whether anemia was arising as a result of decreased red blood cell production, we harvested bone marrow cells and costained for CD71 and TER119 to delineate the different stages of erythropoietic development. Previous groups have utilized this method to show that mice deficient in B12 and FA uptake present with an accumulation in late basophilic and chromatophilic erythroblasts in gate 3 (G3) (24, 25). Strikingly, we observed a similar accumulation of G3 erythroblasts in mice treated with TCDD alone, suggesting a common underlying mechanism as B12/FA deficiency. We further observed that cotreatment of DMB or PABA reversed this accumulation (Fig. 3C and D).

We observed a similar rescue phenotype with DMB and PABA when assessing hepatic steatosis. TCDD has long been known to induce fatty liver disease in mice (21), and similarly, B12 and FA levels have been reported to inversely correlate to the severity of fatty liver disease—without a clear explanation of how (7). In our studies, mice treated with TCDD long-term presented with increased retention of fat droplets in the liver compared to mice treated with DMB and PABA (Fig. 3E).

Last, we evaluated the effect of DMB and PABA in alleviating birth defects induced by TCDD. TCDD prototypically induces cleft palate in mice (19), and it is thought to do so by inhibiting FGFR1 or TGFB3 during the elevation and fusion stages of palatal development (26, 27). In human patients, on the other hand, it is already known clinically that B12 and FA supplementation can decrease the incidence of cleft lip and cleft palate (5). Providing a mixture treatment of DMB and PABA to pregnant mice, we observed a significant decrease in the incidence of cleft palate, compared to mice receiving TCDD alone at embryonic day 10.5 (E10.5) (Fig. 3F and *SI Appendix*, Fig.

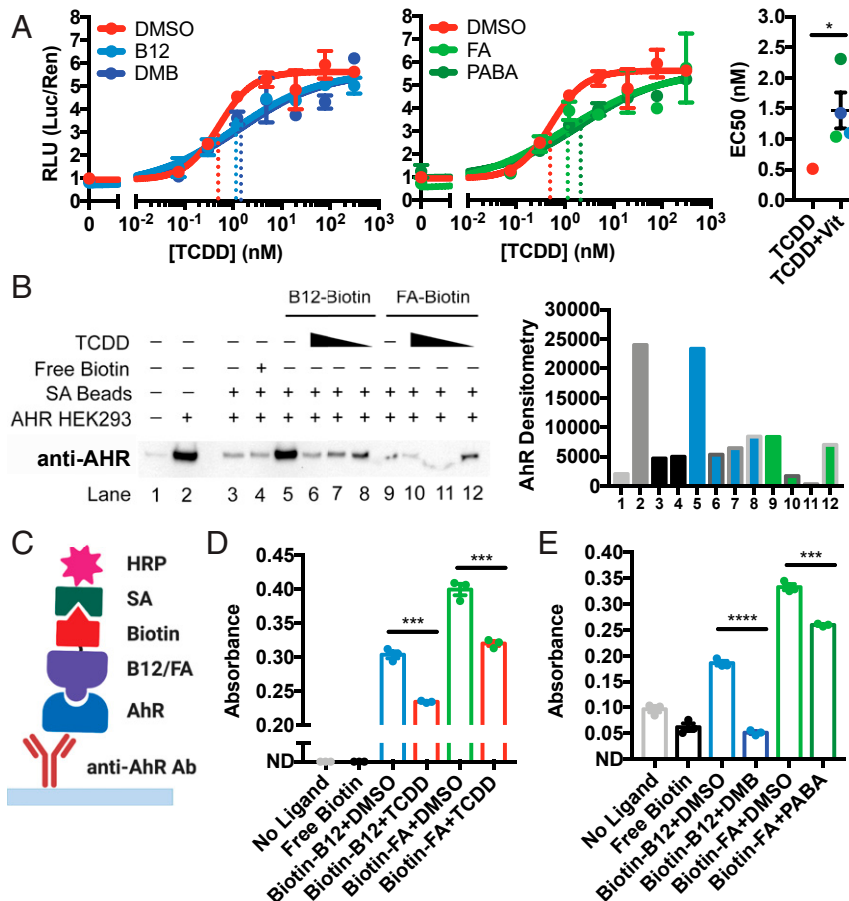


Fig. 2. B12 and FA bind directly to AhR, competing with TCDD, via DMB and PABA. (A) Dual luciferase assay of HepG2 cells treated with serial dilutions of TCDD in the presence of 1,000 pg/mL B12 (with 1 pM TCN2), 0.68 nM DMB, 10 ng/mL FA, or 22.6 nM PABA for 24 h. Same experiment is shown in two separate graphs for clarity. RLUs were calculated by normalizing firefly luciferase signal with *Renilla* luciferase signal within each sample and further normalizing with DMSO-treated samples. After data were fitted with nonlinear regression in GraphPad Prism, EC₅₀ for each dose–response curve was plotted. The dashed lines indicate location of EC₅₀. Data are means ± SE (*n* = 3). **P* < 0.05 vs. TCDD-treated EC₅₀ assessed by Student’s *t* test. (B) Lysates from HEK293T cells over-expressing human AhR were incubated with streptavidin (SA) beads complexed with biotinylated-B12/FA in the presence of DMSO or serial dilutions of TCDD (10, 1, 0.1 nM). Bound protein was eluted and subjected to Western blotting for AhR. Densitometry of bands was quantified by ImageJ. (C) Overview of ELISA-based binding assay. Diagram generated using BioRender. (D and E) Plates coated with anti-AhR antibody were incubated overnight with overexpressed AhR lysate from HEK293T. Plates were then incubated with biotinylated B12/FA in the presence of (D) TCDD or (E) DMB and PABA for 1 h. After incubation with SA-conjugated HRP, samples were developed with TMB substrate for 30 min. Absorbances were measured by microplate reader and adjusted by subtracting absorbances at 490 nm from absorbances at 450 nm. Data are means ± SE (*n* = 3). ****P* < 0.001, *****P* < 0.0001 vs. DMSO-treated samples assessed by Student’s *t* test.

S4C). In sum, these results demonstrate that Vitamin B12 and FA alleviate hallmark symptoms of nutritional deficiency replicated by AhR overactivation.

B12 and FA Deficiencies Induce Transcriptional Changes and Hematologic Symptoms in an AhR-Dependent Manner. To assess whether B12/FA deficiency is able to induce AhR transcriptional activity, we fed special diets to mice for a period of 16 wk and confirmed that homocysteine levels were significantly elevated, an early marker of functional B12/FA depletion indicating disruption in the 1C cycle (Fig. 4A). Consistent with prior reports showing that FA-deficient mice have higher *Cyp11a1* mRNA expression at baseline (28), our B12 and FA-deficient mice exhibited elevated liver *Cyp11a1* mRNA (Fig. 4B) and accumulation of G3 erythroblasts (Fig. 4C) at levels comparable to control diet-fed mice treated once with a small dose of TCDD.

Through the use of AhR-null mice, which are unresponsive to TCDD treatment (Fig. 4D), we further found that *Cyp11a1* mRNA induction and erythroblast accumulation from FA deficiency are dependent on functional AhR (Fig. 4E and F). Given prior reports that B12 and FA deficiency results in global

hypomethylation and up-regulation of retroelements (29, 30), we also examined transcription of LINE1 retroelements. Surprisingly, we found that the relative LINE1 induction caused by FA-deficient diets was also abrogated with AhR deficiency (*SI Appendix, Fig. S6*). These results suggest more generally, then, that the transcriptional changes and symptoms arising from B12 and FA deficiency may in fact be mediated through AhR signaling.

Mutations in B12/FA Uptake Correlate with Induction in AhR Target Genes and Repression of Pathways Implicated in Birth Defects. Last, we were interested in assessing how relevant this model might be in humans. To do so, we exploited the expansive RNA and DNA sequencing available through The Cancer Genome Atlas (TCGA) PANCAN database. Using batch-normalized data available through University of California, Santa Cruz (UCSC) Xena Browser’s online platform, we first assessed which samples harbored nonsilent mutations in genes encoding B12/FA uptake pathway proteins (*SI Appendix, Fig. S7A*) as a proxy for cellular B12/FA deficiency. Then, we calculated an AhR transcriptional activity score (“AHR score”) using the log₂ normalized expression of five core transcriptional

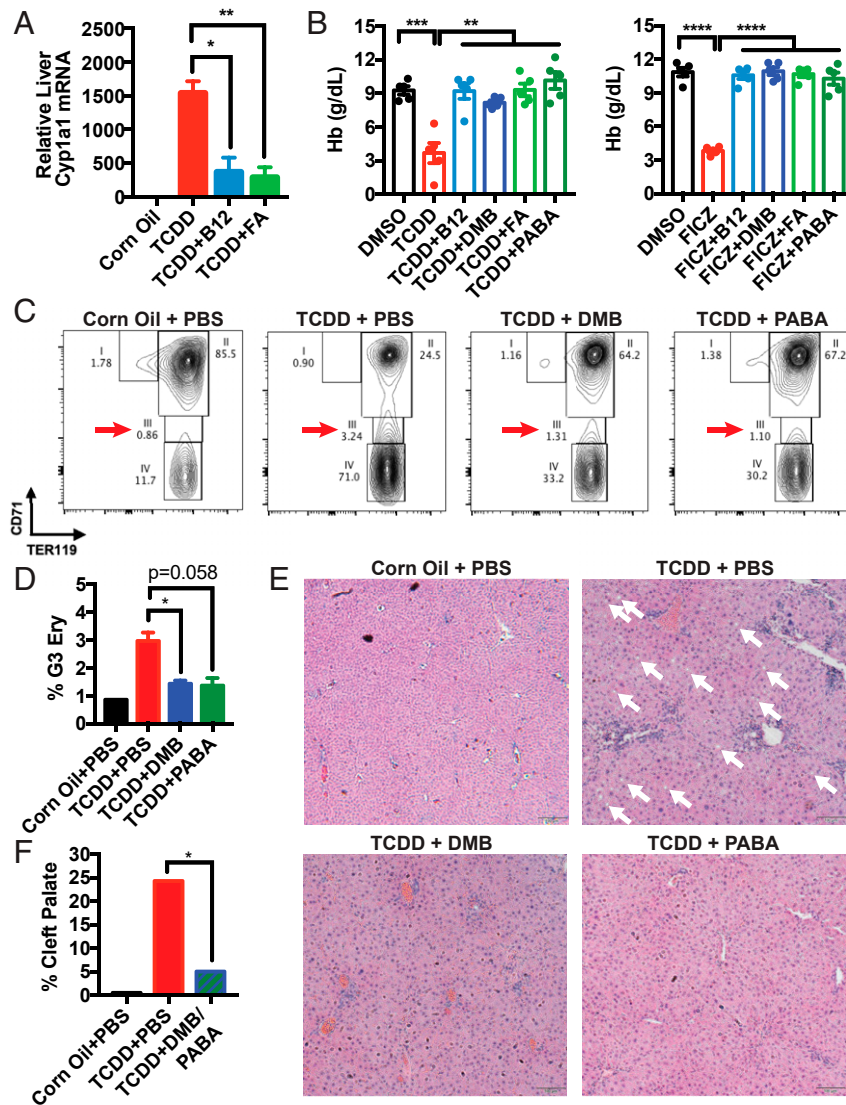


Fig. 3. B12 and FA inhibit AhR activity in vivo and rescue mice from symptoms of deficiency induced by TCDD. (A) B6 mice were intraperitoneally (i.p.) injected with PBS, 1.25 $\mu\text{g}/\text{kg}$ B12, or 12.5 $\mu\text{g}/\text{kg}$ FA and orally administered corn oil or 2 $\mu\text{g}/\text{kg}$ TCDD. RNA was extracted from livers 5 h later. Liver *Cyp1a1* mRNA was measured by RT-qPCR and normalized by *Hprt1* and vehicle control-treated mice. Data are means \pm SE ($n = 4-5$). * $P < 0.05$, ** $P < 0.01$ vs. TCDD-treated mice assessed by Student's *t* test. (B) B6 mice were i.p. injected every day with corn oil, 2 $\mu\text{g}/\text{kg}$ TCDD, or 12.5 $\mu\text{g}/\text{kg}$ FICZ alongside PBS, 12.5 $\mu\text{g}/\text{kg}$ B12, 9.3 nmol/kg DMB, 2.5 mg/kg FA, or 5.7 $\mu\text{mol}/\text{kg}$ PABA. On day 7, hemoglobin (Hb) of retroorbital bleeds was measured by an automatic CBC analyzer. Data are means \pm SE ($n = 5$). *** $P < 0.01$, **** $P < 0.001$, ***** $P < 0.0001$ vs. DMSO- and TCDD-treated mice assessed by Student's *t* test. (C-E) B6 mice were orally administered corn oil or 30 $\mu\text{g}/\text{kg}$ TCDD on a weekly basis and i.p. injected with PBS, 93 nmol/kg DMB, or 56.6 $\mu\text{mol}/\text{kg}$ PABA (equivalent to 50 times estimated daily intake of B12 and FA) every day for 6 wk. (C) Femur bone marrow cells were collected, stained with CD71-APC and TER119-FITC, and analyzed with a flow cytometer. After gating for nondebris TER119⁺ singlets, rectangular gates were drawn to delineate the four stages of erythropoiesis, going from least mature (gate 1) to most mature (gate 4). (D) Proportion of TER119⁺ singlets that are gate 3 (G3) erythroblasts. Data are means \pm SE ($n = 2$). * $P < 0.05$ vs. TCDD-treated mice assessed by Student's *t* test. (E) H&E staining of liver sections collected at the end of week 6, taken at 10 \times magnification. The white arrows indicate fat droplets. (F) B6 female mice were mated with male mice overnight. After visualization of vaginal plugs (day E0.5), mice were orally administered PBS or 37.2 nmol/kg DMB with 22.7 $\mu\text{mol}/\text{kg}$ PABA (20 times estimated daily intake of B12 and FA) every day starting on day E9.5. On day E10.5, mice were orally administered a one-time dose of corn oil or 30 $\mu\text{g}/\text{kg}$ TCDD. Embryos were collected on day E18.5 and assessed for palatogenesis. Incidence of cleft palates was quantified from five to six litters from each arm. * $P < 0.05$ vs. TCDD-treated mice assessed by Z test for population proportions.

targets (*SI Appendix, Fig. S7B*) (31). Doing so, we found that samples harboring mutations in certain proteins of the B12/FA pathway—including *TCN2* (which encodes a necessary B12 carrier protein) and *SLC46A1* (which encodes PCFT, a folate transporter)—had a significantly higher AHR score compared to nonmutated samples (Fig. 5A and *SI Appendix, Fig. S7C*). Quantifying the total number of mutations harbored in these uptake pathways, we observed a seemingly dose-dependent increase in the AHR score. To test the alternative hypothesis that this induction in AhR transcription

is simply being mediated through interruptions in 1C metabolism, we repeated this analysis looking at mutations in enzymes of the 1C cycle that interact directly with B12/FA, and we did not find any comparable inductions in AHR score (Fig. 5B).

Next, to see whether AhR might be involved in birth defects arising from B12 and FA deficiency, we calculated a birth defect transcriptional score (“BD score”) that summarizes log₂ expression of pathways suppressed by AhR whose deficiencies have already been implicated in the pathogenesis of major birth defects

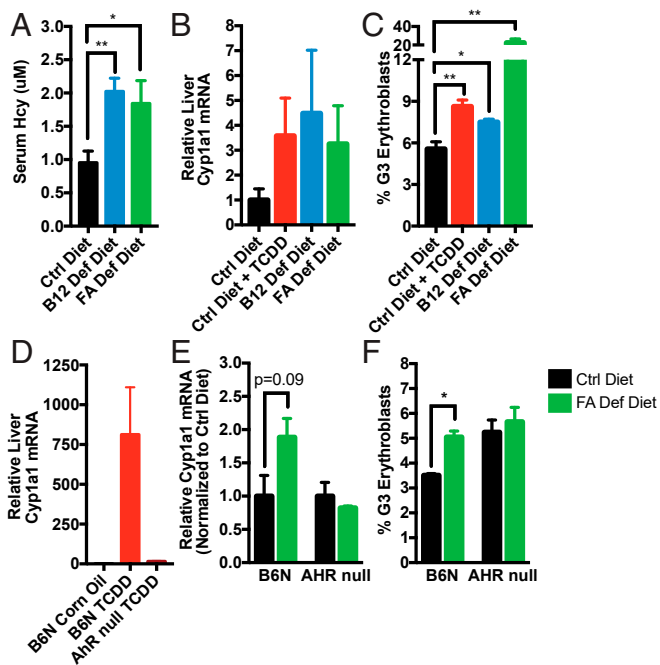


Fig. 4. B12 and FA deficiency may induce *Cyp1a1* mRNA in liver and accumulation of erythroblasts in bone marrow in an AhR-dependent manner. (A–C) B6 mice were fed control, B12-deficient, or FA-deficient diets for 16 wk on wire bottom cages. (A) Serum homocysteine (Hcy) was measured in retro-orbital blood by commercial fluorometric kit. After confirming depletion of B12/FA, half of control diet-fed mice were orally administered 10 ng/kg TCDD overnight and all other mice received corn oil. Mice livers and bone marrows were collected and processed the following day. (B) Relative liver *Cyp1a1* mRNA measured by RT-qPCR and normalized to *Hprt1* and corn oil-treated mice. (C) Proportion of TER119⁺ singlets in bone marrow that are G3 erythroblasts, as determined by flow cytometry. Data are means \pm SE ($n = 5$). * $P < 0.05$, ** $P < 0.01$ vs. control diet-fed mice assessed by Student's t test. (D) B6 and AHR-null mice were injected i.p. with corn oil or 2 μ g/kg TCDD. After 5 h, livers were processed for analysis. Relative liver *Cyp1a1* mRNA was measured by RT-qPCR and normalized to *Hprt1* and corn oil-treated mice. Data are means \pm SE ($n = 2-3$). (E and F) B6 and AHR-null mice were fed control or FA-deficient diet for 8 wk on wire bottom cages. (E) Relative liver *Cyp1a1* mRNA measured by RT-qPCR and normalized to *Hprt1* and control diet-fed mice. (F) Proportion of G3 erythroblasts among TER119⁺ singlets in bone marrow, as determined by flow cytometry. Data are means \pm SE ($n = 3-4$). * $P < 0.05$ vs. control diet-fed mice assessed by Student's t test.

(SI Appendix, Fig. S7B) (26, 27, 32–34). Consistent with the activation of AhR signaling seen previously (Fig. 5B), samples with mutated B12/FA uptake pathways produced significantly lower BD scores for all evaluated B12/FA uptake genes and, when taken in aggregate, revealed a dose-dependent effect of mutations in these pathways (Fig. 5C and SI Appendix, Fig. S7D). Strikingly, when this analysis was repeated for samples mutated in the 1C cycle, there was no difference observed between mutated and nonmutated samples as with AHR scores (Fig. 5D), supporting the notion that birth defect pathogenesis may not simply be a downstream effect of faulty DNA synthesis.

Discussion

We report here that vitamin B12 and FA function as naturally occurring antagonists of AhR. B12 and FA bind AhR directly as competitive antagonists, blocking AhR nuclear localization, XRE binding, and target gene up-regulation mediated by AhR agonists like TCDD and FICZ. In mice, TCDD treatment replicated many of the hallmark symptoms of B12/FA deficiency, including anemia and cleft palate formation, and cotreatment with vitamin DMB and PABA rescued mice from these toxic

effects. Moreover, we found that B12/FA deficiency in mice induces AhR transcriptional activity and accumulation of erythroid progenitors and that it may do so in an AhR-dependent fashion. Consistent with our animal and in vitro work, we observed that human cancer samples with mutated B12/FA uptake proteins demonstrated higher transcription of AhR target genes and lower transcription of pathways implicated in birth defects. Notably, there was no significant difference in these pathways when considering samples with mutated 1C cycle enzymes, suggesting that symptoms of deficiency might not be a result of faulty DNA synthesis, as it is currently thought.

To our knowledge, B12 and FA currently represent the only naturally occurring AhR antagonists that 1) bind AhR with high affinity (with EC₅₀ values in the nanomolar ranges) and 2) are present at biologically relevant concentrations. In contrast, resveratrol, perhaps the most well-known natural AhR antagonist, has a reported EC₅₀ of 6 μ M and is far from ubiquitous in the human body, present most prominently in red wine (35). Similarly, while nicotinamide (a constituent of vitamin B3) has been shown to have some antagonistic properties on AhR toxicity (36), it has not yet been shown to directly bind AhR and, furthermore, demonstrates in vitro efficacy only at millimolar concentrations. Hence, especially when we consider the preponderance of natural AhR agonists (37) alongside the current lack of effective antagonists, B12 and FA appear to fill a necessary teleological role of counteracting AhR overstimulation that would otherwise occur at baseline.

Synthesizing these concepts with our findings, then, we propose a working model for how vitamin B12 and FA may be functioning in both physiologic and pathologic contexts (Fig. 5E). In healthy adults, we believe that B12 and FA effectively blunt AhR activation by various agonists that we are constantly exposed to by means of endogenous production, diet, or toxic exposure to xenobiotics. What ultimately results from this balance of antagonists and agonists is tonic AhR signaling that helps to promote homeostasis and physiological processes. However, under B12- or FA-deficient contexts (which can commonly arise through veganism, pregnancy, or age-related malabsorption), naturally occurring agonists can saturate AhR binding and overactivate the signaling pathway, leading to many of the same symptoms that can be observed with AhR dysregulation.

Interestingly, we observed that extremely high doses of B12/FA yielded worse inhibition than physiologically relevant concentrations, particularly for B12 and DMB (SI Appendix, Fig. S1). While further studies to confirm this effect are warranted, this relationship appears to mimic the biphasic dose–response curve observed with some AhR ligands with antagonistic properties, like ANP and BNP (38). In these cases, it is thought that, at lower concentrations, these ligands engage higher-affinity antagonistic pockets within the LBD, but at higher concentrations, these ligands can also interact with lower-affinity agonistic sites. This complex dynamic with AhR, then, may ultimately help to explain the “U-shaped” relationship that has been widely observed between B12/FA levels and various forms of morbidity (39), a phenomenon that has not been sufficiently explained by the 1C cycle alone.

By purporting that symptoms of vitamin-deficient patients are ultimately driven by the dominant AhR ligand present—and not by B12/FA deficiency alone—our model also helps to explain some of the stochasticity that is observed clinically, especially in the context of birth defects. Owing to the open nature of its LBD, AhR is known to elicit slightly different transcriptional responses and phenotypes depending on the structure of the agonist. In the case of murine birth defects, for instance, some AhR agonists (like TCDD) characteristically induce cleft palates, while others may induce neural tube defects (27, 40). In the context of human patients, then, our model would predict that the actual birth defect observed in the vitamin-deficient mother actually depends on the particular mix of agonists that is determined by her diet and

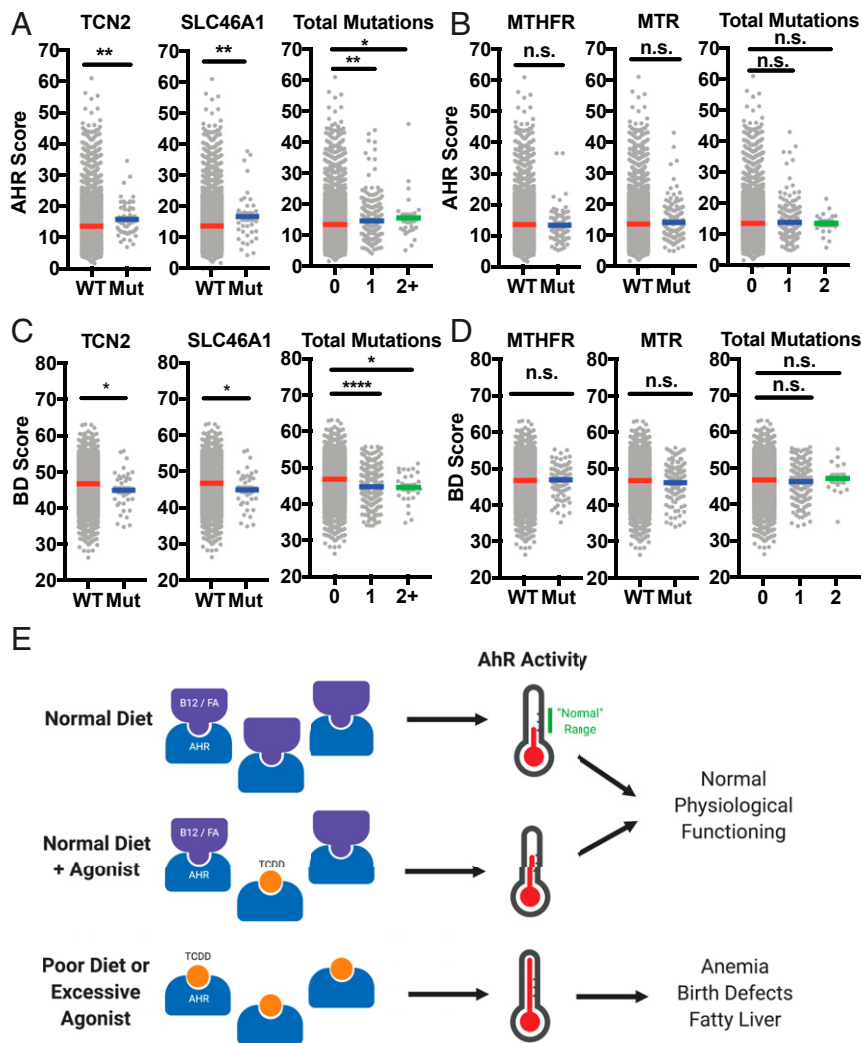


Fig. 5. Deficiency in B12 and FA uptake, but not in 1C metabolism, is associated with induction in AhR activity and repression in pathways associated with birth defect. (A) AHR score (calculated from the log₂-normalized expression of AhR target genes listed in *SI Appendix, Fig. S6B*) for TCGA samples with and without nonsilent mutations in B12 uptake gene *TCN2* (Left) and FA uptake gene *SLC46A1* (Center). AHR score was also calculated based on the number of genes mutated in the B12/FA uptake pathway (Right). (B) AHR score for samples with and without nonsilent mutations in *MTHFR* (Left) and *MTR* (Right) encoding 1C cycle enzymes. AHR score was also calculated based on the number of mutations present between these two genes (Right). (C) BD score (calculated from the log₂-normalized expression of genes implicated in birth defects and identified as repressed targets of AhR activation, listed in *SI Appendix, Fig. S6B*) for TCGA samples with and without mutations in *TCN2* and *SLC46A1*. BD score was also calculated based on the number of gene mutated in the B12/FA uptake pathway (Right). (D) AHR score for samples with and without nonsilent mutations in *MTHFR* (Left) and *MTR* (Right). AHR score was also calculated based on the number of mutations present between these two genes (Right). (E) Proposed model for how B12 and FA may be preventing symptoms arising from overactivation of AhR. **P* < 0.05, ***P* < 0.01, *****P* < 0.0001, and n.s., not significant, vs. nonmutated samples assessed by Student's *t* test.

environmental exposures (41). In contrast to this rationale, the currently accepted model posits that deficiency of the vitamins alone (by blocking DNA synthesis) should be sufficient in producing symptoms. This model, then, would predict that, similar to the MS homozygous knockout mice exhibiting 100% embryonic lethality (13), birth defects in human patients would present more deleteriously and homogeneously than are actually observed.

Our model also might help explain a previously puzzling finding that FA-deficient diets alone are not sufficient in producing birth defects in mice (42). Indeed, the fact that laboratory mice are not normally exposed to common sources of AhR agonists—like UV radiation or diet (43)—may yield a smaller pool of AhR agonists at baseline and blunt the consequences unmasked by vitamin deficiency. Consistent with this reasoning, we observed that *Cyp1a1* induction in B12/FA-deficient mice was generally less robust than the induction seen with toxic doses of TCDD (Figs. 3A and 4D).

Beyond the classical symptoms of vitamin B12/FA deficiency, this model can also lend insight into other symptoms and comorbidities associated with AhR dysregulation. Hyperpigmentation, for instance, has been well described with B12 deficiency among darker-skinned individuals (44), but no clear explanation of mechanism currently exists. Given how AhR mediates the UV pigmentation response and regulates melanogenesis (45, 46), our study suggests a possibility that B12/FA deficiency might confer more sensitivity to pigmentation-promoting AhR agonists like FICZ. In another example, symptoms of major depression have been noted to correlate with levels of kynurenine, another AhR agonist (47), while B12/FA deficiencies often present as comorbidities in depressive patients (48). Considering how B12 supplementation has already proven beneficial for depression in some clinical trials (49), it may be possible then that B12/FA are modulating depressive symptoms through the AhR axis.

In conclusion, our data demonstrate that B12 and FA directly engage a signaling pathway distinct from the 1C cycle. The resulting model not only provides a far more parsimonious explanation for the symptoms of deficiency that are observed clinically, but also underscores the prevailing importance of AhR signaling in the maintenance of homeostatic and developmental processes in healthy individuals.

Materials and Methods

Reagents and Antibodies. Vitamin B12 (V2876), DMB (D147206), folic acid (F7876), PABA (A9878), FICZ (SML1489), and BaP (B1760) were purchased from Sigma-Aldrich. TCDD (D-4045-DMSO-10X) was purchased from AccuStandard. Dynabeads MyOne T1 Streptavidin beads (65601) were purchased from Thermo Fisher Scientific. Biotin-PEG-B12 (PG2-B12BN-5k) and Biotin-PEG-FA (PG2-BNFA-5k) were purchased from Nanocs. FITC anti-TER119 antibody (116206), APC anti-CD71 antibody (113820), and SA-HRP (405210) were purchased from BioLegend. Anti-AhR WB/ELISA (sc-133088) and anti-HDAC1 (sc-7872) antibodies were purchased from Santa Cruz Antibody. Anti-AhR ChIP antibody (832005) was purchased from Cell Signaling Technologies. Recombinant human TCN2 (MBS1123820) was purchased from MyBioSource.

Plasmids and Cell Lines. Human AhR plasmid (SC119159) was purchased from OriGene. Plasmids pGL4.43 XRE-luc2P (PRE4121) and pGL4.75 CMV-Ren (PRE6931) were purchased from Promega. HepG2 cells (HB-8065) were purchased from ATCC.

Mice. C57BL/6 (B6) were purchased from Charles River Laboratories and subsequently bred and housed at Yale University. B6 mice harboring the nonresponsive *Ahr^d* allele (AhR null) were a gift from R.M. (50). Mice were maintained in our facility until the ages described. Sex-matched, 5- to 8-wk-old mice were used for all experiments. All procedures used in this study complied with federal and institutional policies of the Yale Animal Care and Use Committee. The study was approved by an institutional review board.

Vitamin-Deficient Diet Experiments. FA-deficient diet with 1% succinylsulfathiazole (TD.01505), B12-deficient diet with 5% pectin (TD.190092), and corresponding control diets (TD.110166, TD.190091) were purchased from Envigo. Female mice were provided special diets and housed in cages with wire bottoms to prevent coprophagy. At the end of the designated depletion period, blood was collected retroorbitally under isoflurane anesthesia. Total homocysteine in prepared plasma was measured using a commercial fluorometric kit (Abcam; ab228559) to confirm successful depletion.

TCGA Analysis. Somatic mutation and batch-normalized mRNA expression data from TCGA Pan-Cancer (PANCAN) database were downloaded using the UCSC Xena Browser (<https://xenabrowser.net/>). Samples with missing entries were removed from analysis. Missense, nonsense, and frameshift mutations were coded as nonsilent mutations. Expression of AhR target genes and birth defect genes (*SI Appendix, Fig. S7B*) were totaled to calculate AHR score and BD score, respectively. Data were stratified based on mutation status of B12/FA uptake genes and 1C enzyme genes (*SI Appendix, Fig. S7A*), and expression scores were plotted in GraphPad Prism.

ELISA Binding Assay. ELISA plates were coated with anti-AhR antibody (1:50) in bicarbonate coating buffer (50 mM carbonate-bicarbonate, pH 9.6) overnight at 4 °C. After plates were washed twice with TNT buffer (0.1 M Tris-HCl, pH 7.5, 0.15 M NaCl, 0.05% Tween 20), plates were blocked for 2 h at room temperature (RT) in 5% FBS (in PBS). HEK293T transfected with AhR overexpression plasmid were lysed in RIPA buffer (150 mM NaCl, 1% Nonidet P-40, 0.5% DOC, 0.1% SDS, 25 mM Tris, pH 7.4, protease inhibitor, phosphatase inhibitor) and incubated on ice for 30 min. After centrifugation at 15,000 rpm for 15 min at 4 °C, lysate was diluted 1:100 in blocking buffer and incubated in ELISA plate overnight at 4 °C. After plates were washed three times in TNT buffer, biotinylated ligand and competing ligand were added to each well and incubated for 1 h at RT. Plates were washed three times in TNT buffer and incubated with SA-HRP (1:200) for 1 h at RT. After

three more washes in TNT buffer, TMB substrate (eBioscience; 00-4201-56) was added to each well and incubated for 30 min. Reaction was quenched with stop solution (2 N H₂SO₄), and plate was read at 450 and 490 nm (background) in a microplate reader.

B12/FA Pull-Down Assay. Biotinylated-B12 and FA were conjugated to streptavidin T1 Dynabeads at RT for 30 min in DB buffer (20 mM Tris-HCl, pH 8.0, 2 M NaCl, 0.5 mM EDTA, 0.03% Nonidet P-40). After one wash in DB buffer and three washes in PB buffer (50 mM Tris-HCl, pH 8.0, 150 mM NaCl, 10 mM MgCl₂, 0.5% Nonidet P-40, proteinase inhibitor), beads were then incubated with lysate from HEK293T overexpressing AhR alongside competing ligands for 2 h. Beads were washed four times with PB buffer, and bound proteins were eluted by boiling samples in SDS loading buffer. Proteins were subjected to immunoblotting, as described elsewhere.

Flow Cytometry. Bone marrow progenitors were harvested by flushing out femurs with RPMI media supplemented with 10% FBS using a 27G needle and passed through 70- μ m filter. Samples were centrifuged at 1,500 rpm at 4 °C for 5 min and washed with PBS. Cells were incubated with Fc block (clone 2.4G2) for 15 min in 4 °C and washed with FACS buffer (PBS with 5% FBS). Cells were incubated with anti-TER119 and anti-CD71 antibodies for 30 min in 4 °C. Cells were washed with FACS buffer and resuspended in 1% PFA. Samples were run on BD LSR II, and data were analyzed by FlowJo. After gating for nondebris TER119⁺ singlets, rectangular gates were drawn to delineate the four stages of erythropoiesis, going from least mature (gate 1) to most mature (gate 4). Proportion of cells in gate 3 (G3) was calculated for each sample.

Cleft Palate Analysis. Female B6 mice were mated with male mice overnight. After visualization of vaginal plugs (day E0.5), mice were orally administered PBS or 37.2 nmol/kg DMB with 22.7 μ mol/kg PABA (20 times estimated daily intake of B12 and FA) every day starting on day E9.5. On day E10.5, mice were orally administered a one-time dose of corn oil or 30 μ g/kg TCDD. Embryos were collected on day E18.5 and dissected under a light microscope. Lower jaw was removed to visualize palatal formation.

Dual Luciferase Assays. During serum starvation, HepG2 cells were cotransfected with pGL4.43 XRE-luc2P and pGL4.75 CMV-Ren at a 9:1 ratio using Lipofectamine 2000 (Thermo Fisher Scientific). After treatment with compounds, cells were lysed using signals from firefly and *Renilla* luciferase were measured using Dual Luciferase Reporter Assay (Promega) and microplate reader. Relative luciferase units (RLU) were calculated by normalizing firefly luciferase signal with *Renilla* luciferase signal, followed by normalization with vehicle-control-treated sample.

Statistical Analysis. For statistical analysis, the data were analyzed by Student's *t* test or *Z* test of population proportions (GraphPad Prism) as indicated in each figure legend. A *P* value of less than 0.05 is considered statistically significant.

Data Availability. No new sequencing data were generated for this study. Somatic mutation data and normalized RNA-seq data from the TCGA Pan-Cancer dataset (PANCAN) can be downloaded directly with UCSC Xena Browser (<https://xenabrowser.net/>). All other pertinent data are included in the manuscript.

ACKNOWLEDGMENTS. We thank Manabu Taura, Karen Agaronyan, and Zuri Sullivan for their valuable suggestions related to experimental design and providing necessary materials. Research in our laboratory is supported by National Institutes of Health (NIH) Grants 1R01AI127429, 75N93019C00051, 1R01NS111242, and 2U19AI089992 (to A.I.). A.I. is an Investigator of the Howard Hughes Medical Institute. D.J.K. was a Paul and Daisy Soros Fellow and was supported in part by a grant from the National Cancer Institute of the NIH (F30CA236466). D.J.K. and J.K. were supported by Medical Scientist Training Program grants from the NIH (T32GM007205; T32GM136651). S.S.T. was supported by a grant from the National Institute of Diabetes and Digestive and Kidney Diseases of the NIH (T35DK104689).

1. B. N. Ng'eno *et al.*, High prevalence of vitamin B12 deficiency and no folate deficiency in young children in Nepal. *Nutrients* **9**, 72 (2017).
2. L. M. Rogers *et al.*, Global folate status in women of reproductive age: A systematic review with emphasis on methodological issues. *Ann. N. Y. Acad. Sci.* **1431**, 35–57 (2018).
3. E. Andrés *et al.*, Vitamin B12 (cobalamin) deficiency in elderly patients. *CMAJ* **171**, 251–259 (2004).

4. D. S. Socha, S. I. DeSouza, A. Flagg, M. Sekeres, H. J. Rogers, Severe megaloblastic anemia: Vitamin deficiency and other causes. *Cleve. Clin. J. Med.* **87**, 153–164 (2020).
5. J. Schubert, R. Schmidt, E. Syska, B group vitamins and cleft lip and cleft palate. *Int. J. Oral Maxillofac. Surg.* **31**, 410–413 (2002).
6. A. M. Molloy, P. N. Kirke, L. C. Brody, J. M. Scott, J. L. Mills, Effects of folate and vitamin B12 deficiencies during pregnancy on fetal, infant, and child development. *Food Nutr. Bull.* **29** (suppl. 2), S101–S111, discussion S112–S115 (2008).

7. M. Mahamid *et al.*, Folate and B12 levels correlate with histological severity in NASH patients. *Nutrients* **10**, 440 (2018).
8. S. D. Grosse, R. J. Berry, J. Mick Tilford, J. E. Kucik, N. J. Waitzman, Retrospective assessment of cost savings from prevention: Folic acid fortification and spina bifida in the U.S. *Am. J. Prev. Med.* **50** (suppl. 1), S74–S80 (2016).
9. D. S. Froese, B. Fowler, M. R. Baumgartner, Vitamin B₁₂, folate, and the methionine remethylation cycle-biochemistry, pathways, and regulation. *J. Inherit. Metab. Dis.* **42**, 673–685 (2019).
10. A. Imbard, J. F. Benoist, H. J. Blom, Neural tube defects, folic acid and methylation. *Int. J. Environ. Res. Public Health* **10**, 4352–4389 (2013).
11. B. Celtikci *et al.*, Altered expression of methylenetetrahydrofolate reductase modifies response to methotrexate in mice. *Pharmacogenet. Genomics* **18**, 577–589 (2008).
12. D. Li, L. Pickell, Y. Liu, R. Rozen, Impact of methylenetetrahydrofolate reductase deficiency and low dietary folate on the development of neural tube defects in splotch mice. *Birth Defects Res. A Clin. Mol. Teratol.* **76**, 55–59 (2006).
13. D. A. Swanson *et al.*, Targeted disruption of the methionine synthase gene in mice. *Mol. Cell. Biol.* **21**, 1058–1065 (2001).
14. K. Kawajiri, Y. Fujii-Kuriyama, The aryl hydrocarbon receptor: A multifunctional chemical sensor for host defense and homeostatic maintenance. *Exp. Anim.* **66**, 75–89 (2017).
15. Y. L. Guo, M. L. Yu, C. C. Hsu, W. J. Rogan, Chloracne, goiter, arthritis, and anemia after polychlorinated biphenyl poisoning: 14-year follow-up of the Taiwan Yucheng cohort. *Environ. Health Perspect.* **107**, 715–719 (1999).
16. L. Wang *et al.*, 2,3,7,8-Tetrachlorodibenzo-p-dioxin (TCDD) induces peripheral blood abnormalities and plasma cell neoplasms resembling multiple myeloma in mice. *Cancer Lett.* **440–441**, 135–144 (2019).
17. J. D. Erickson *et al.*, Vietnam veterans' risks for fathering babies with birth defects. *JAMA* **252**, 903–912 (1984).
18. F. M. Moran *et al.*, Effects of 2,3,7,8-tetrachlorodibenzo-p-dioxin (TCDD) on fatty acid availability and neural tube formation in cynomolgus macaque, *Macaca fascicularis*. *Birth Defects Res. B Dev. Reprod. Toxicol.* **71**, 37–46 (2004).
19. T. N. Takagi, K. A. Matsui, K. Yamashita, H. Ohmori, M. Yasuda, Pathogenesis of cleft palate in mouse embryos exposed to 2,3,7,8-tetrachlorodibenzo-p-dioxin (TCDD). *Teratog. Carcinog. Mutagen.* **20**, 73–86 (2000).
20. C. C. Lee, Y. J. Yao, H. L. Chen, Y. L. Guo, H. J. Su, Fatty liver and hepatic function for residents with markedly high serum PCDD/Fs levels in Taiwan. *J. Toxicol. Environ. Health A* **69**, 367–380 (2006).
21. J. H. Lee *et al.*, A novel role for the dioxin receptor in fatty acid metabolism and hepatic steatosis. *Gastroenterology* **139**, 653–663 (2010).
22. B. Zhao, D. E. Degroot, A. Hayashi, G. He, M. S. Denison, CH223191 is a ligand-selective antagonist of the Ah (Dioxin) receptor. *Toxicol. Sci.* **117**, 393–403 (2010).
23. C. A. Bradfield, A. Poland, A competitive binding assay for 2,3,7,8-tetrachlorodibenzo-p-dioxin and related ligands of the Ah receptor. *Mol. Pharmacol.* **34**, 682–688 (1988).
24. K. V. Salojin *et al.*, A mouse model of hereditary folate malabsorption: Deletion of the PCFT gene leads to systemic folate deficiency. *Blood* **117**, 4895–4904 (2011).
25. Z. Zhou *et al.*, MCP1P1 deficiency in mice results in severe anemia related to auto-immune mechanisms. *PLoS One* **8**, e82542 (2013).
26. T. L. Thoma, E. A. Stevens, C. A. Bradfield, Transforming growth factor-beta3 restores fusion in palatal shelves exposed to 2,3,7,8-tetrachlorodibenzo-p-dioxin. *J. Biol. Chem.* **280**, 12742–12746 (2005).
27. K. Fujiwara, T. Yamada, K. Mishima, H. Imura, T. Sugahara, Morphological and immunohistochemical studies on cleft palates induced by 2,3,7,8-tetrachlorodibenzo-p-dioxin in mice. *Congenit. Anom. (Kyoto)* **48**, 68–73 (2008).
28. J. Zhang *et al.*, NADPH-cytochrome P-450 reductase, cytochrome P-450 2C11 and P-450 1A1, and the aryl hydrocarbon receptor in livers of rats fed methyl-folate-deficient diets. *Nutr. Cancer* **28**, 160–164 (1997).
29. S. Chang *et al.*, Long interspersed nucleotide element-1 hypomethylation in folate-deficient mouse embryonic stem cells. *J. Cell. Biochem.* **114**, 1549–1558 (2013).
30. K. Asada *et al.*, LINE-1 hypomethylation in a choline-deficiency-induced liver cancer in rats: Dependence on feeding period. *J. Biomed. Biotechnol.* **2006**, 17142 (2006).
31. T. V. Beischlag, J. Luis Morales, B. D. Hollingshead, G. H. Perdew, The aryl hydrocarbon receptor complex and the control of gene expression. *Crit. Rev. Eukaryot. Gene Expr.* **18**, 207–250 (2008).
32. K. L. Lorick, D. L. Toscano, W. A. Toscano Jr., 2,3,7,8-Tetrachlorodibenzo-p-dioxin alters retinoic acid receptor function in human keratinocytes. *Biochem. Biophys. Res. Commun.* **243**, 749–752 (1998).
33. Z. Andrysiak *et al.*, Aryl hydrocarbon receptor-mediated disruption of contact inhibition is associated with connexin43 downregulation and inhibition of gap junctional intercellular communication. *Arch. Toxicol.* **87**, 491–503 (2013).
34. J. Ya *et al.*, Heart defects in connexin43-deficient mice. *Circ. Res.* **82**, 360–366 (1998).
35. R. F. Casper *et al.*, Resveratrol has antagonist activity on the aryl hydrocarbon receptor: Implications for prevention of dioxin toxicity. *Mol. Pharmacol.* **56**, 784–790 (1999).
36. S. Diani-Moore *et al.*, Identification of the aryl hydrocarbon receptor target gene TiPARP as a mediator of suppression of hepatic gluconeogenesis by 2,3,7,8-tetrachlorodibenzo-p-dioxin and of nicotinamide as a corrective agent for this effect. *J. Biol. Chem.* **285**, 38801–38810 (2010).
37. R. Shinde, T. L. McGaha, The aryl hydrocarbon receptor: Connecting immunity to the microenvironment. *Trends Immunol.* **39**, 1005–1020 (2018).
38. A. A. Soshilov, M. S. Denison, Ligand promiscuity of aryl hydrocarbon receptor agonists and antagonists revealed by site-directed mutagenesis. *Mol. Cell. Biol.* **34**, 1707–1719 (2014).
39. S. Tal, F. Stern, Z. Polyak, I. Ichelzon, Y. Dror, Moderate "multivitamin" supplementation improved folate and vitamin B12 status in the elderly. *Exp. Gerontol.* **84**, 101–106 (2016).
40. S. Lin *et al.*, Oxidative stress and apoptosis in benzo[a]pyrene-induced neural tube defects. *Free Radic. Biol. Med.* **116**, 149–158 (2018).
41. V. Rothhammer, F. J. Quintana, The aryl hydrocarbon receptor: An environmental sensor integrating immune responses in health and disease. *Nat. Rev. Immunol.* **19**, 184–197 (2019).
42. M. K. Heid, N. D. Bills, S. H. Hinrichs, A. J. Clifford, Folate deficiency alone does not produce neural tube defects in mice. *J. Nutr.* **122**, 888–894 (1992).
43. C. Vogeley, C. Esser, T. Tüting, J. Krutmann, T. Haarmann-Stemann, Role of the aryl hydrocarbon receptor in environmentally induced skin aging and skin carcinogenesis. *Int. J. Mol. Sci.* **20**, 6005 (2019).
44. T. T. Chiang, C. T. Hung, W. M. Wang, J. T. Lee, F. C. Yang, Recreational nitrous oxide abuse-induced vitamin B12 deficiency in a patient presenting with hyperpigmentation of the skin. *Case Rep. Dermatol.* **5**, 186–191 (2013).
45. B. Jux *et al.*, The aryl hydrocarbon receptor mediates UVB radiation-induced skin tanning. *J. Invest. Dermatol.* **131**, 203–210 (2011).
46. S. Luecke *et al.*, The aryl hydrocarbon receptor (AHR), a novel regulator of human melanogenesis. *Pigment Cell Melanoma Res.* **23**, 828–833 (2010).
47. D. Liu *et al.*, Beta-defensin 1, aryl hydrocarbon receptor and plasma kynurenine in major depressive disorder: Metabolomics-informed genomics. *Transl. Psychiatry* **8**, 10 (2018).
48. A. J. Levitt, R. T. Joffe, Folate, B12, and life course of depressive illness. *Biol. Psychiatry* **25**, 867–872 (1989).
49. E. U. Syed, M. Wasay, S. Awan, Vitamin B12 supplementation in treating major depressive disorder: A randomized controlled trial. *Open Neurol. J.* **7**, 44–48 (2013).
50. A. Poland, D. Palen, E. Glover, Analysis of the four alleles of the murine aryl hydrocarbon receptor. *Mol. Pharmacol.* **46**, 915–921 (1994).